STRUCTURE AND SOOT PROPERTIES OF NON-BUOYANT LAMINAR

ROUND-JET DIFFUSION FLAMES   N93-20190

Saeed Mortazavi, Peter B. Sunderland, Jongsoo Jurng, and Gerard M. Faeth
Department of Aerospace Engineering
The University of Michigan
Ann Arbor, Michigan 48109-2140

Introduction

The structure and soot properties of nonbuoyant laminar diffusion flames are being studied experimentally and theoretically in order to better understand the soot and thermal radiation emissions from luminous flames. The measurements involve weakly-buoyant flames at low pressures in normal gravity (ng) and nonbuoyant flames at normal pressures in microgravity (μg).

Earlier measurements of the structure of nonbuoyant laminar diffusion flames have used drop towers [1-7]. Measurements have been limited to flame lengths, finding good agreement between predictions based on the conserved-scalar formalism and measurements, although flame length is not a very sensitive indicator of model performance. Additionally, limited instrumentation and test time capabilities of drop towers have inhibited detailed studies of soot processes.

Buoyant laminar diffusion flames have received significant attention [8-20]. However, buoyancy causes soot to be confined to a narrow soot layer that is difficult to resolve experimentally, while the path that soot follows as it grows and oxidizes is completely different in buoyant and nonbuoyant flames [18]. This limits the value of findings from buoyant diffusion flames because nonbuoyant flames are of greatest practical interest. Additionally, Glassman [17] questions the existence of a global property like laminar smoke point flame lengths for nonbuoyant diffusion flames, analogous to buoyant flames, because they have residence times independent of flame length under the boundary layer approximation. Clearly, the mechanism causing practical nonbuoyant flames to emit soot is not understood.

Finally, detailed simulations of chemical kinetics have been successful for methane/air flames where soot concentrations are low [19,20] but analogous methods for soot-containing flames will require substantial advances in the understanding of fuel decomposition and soot chemistry. An alternative approach is possible, however, because gas species concentrations in soot-containing flames are largely functions of the mixture fraction, yielding state relationships that could be used with the conserved-scalar formalism (the laminar flamelet approach). However, this approach has not been tested.

Thus, the objectives of the present investigation are to study the differences of soot properties between nonbuoyant and buoyant diffusion flames, and to evaluate predictions based on the laminar flamelet approach.

Experimental Methods

Normal-Gravity Tests. Detailed measurements of flame properties are being undertaken at ng, exploiting the fact that buoyancy scales like p^2g in laminar flames, where p = pressure (atm.) and g

= normal gravitational acceleration [18]. Thus, flames at pressures of O(0.1 atm.) have effective gravitational levels of O(0.01 g) and are weakly-buoyant if they are not too large. Present measurements were carried out in a windowed chamber using burners having diameters of 3-10 mm with nearly fully-developed laminar pipe flow at the exit. A continuous inflow of fuel and oxidant, and outflow of combustion products, allows unlimited test times. Thus far, measurements include dark-field photography for flame shapes, fine-wire thermocouples for temperature distributions, laser extinction for soot volume fractions, thermophoretic sampling for soot structure, and wide-band radiometry for radiative heat loss fractions, see [8-15] for descriptions of these methods.

Low-Gravity Tests. Tests at μg were carried out to measure the laminar smoke point flame lengths of nonbuoyant laminar jet diffusion flames at pressures of 0.5-2.0 atm. This involved the NASA KC-135 aircraft facility using a test chamber that was designed at NASA-Lewis with burner diameters of 1.6, 2.7 and 5.9 mm, and fully-developed laminar pipe flow at the exit. Measurements were limited to video and film motion pictures of the flames to find laminar smoke point flame lengths.

Theoretical Methods

The following approximations were used to analyze flame structure: steady, laminar, axisymmetric flow; laminar flamelet approximation, which implies equal binary diffusivities of all species, negligible thermal diffusion, unity Lewis number and attached flames; uniform ambient environment; ideal gas mixture with a constant Prandtl/Schmidt number; and constant radiative heat loss fraction of the available chemical energy release. This yields the following governing equations:

$$\nabla \cdot (\rho \, \mathbf{u}) = 0 \tag{1}$$

$$\nabla \cdot (\rho \, \mathbf{u} \, \mathbf{u}) = \rho g - \nabla p + \nabla \cdot (\mu \, (\nabla \mathbf{u} + \nabla \mathbf{u}^T)) \tag{2}$$

$$\nabla \cdot (\rho \, \mathbf{u} \, f) = \nabla \cdot (\mu \, \nabla f)/\sigma \tag{3}$$

where ρ = density, u = velocity vector, μ = viscosity, f = mixture fraction, σ = Prandtl/Schmidt number and superscript T denotes the transpose of a tensor. State relationships giving the composition, temperature, density and viscosity as a function of mixture fraction were found from correlations of measurements in laminar flames for combustion in air [12-14].

Results and Discussion

Flame Structure. Figure 1 is an illustration of predicted and measured flame lengths, L, normalized by the burner diameter, d, as a function of burner exit Reynolds number, Re. These results involve ethylene/air flames at atmospheric pressure, with measurements from Haggard and Cochran [2]. Similar to other evaluations of flame lengths for moderately sooting fuels, the comparison between predictions and measurements is excellent. Flame shapes and temperature distributions provide a more sensitive evaluation of predictions and have been studied using low-pressure flames. Predicted and measured flame shapes for ethylene/air flames at 0.125 and 0.250 atm. are illustrated in Fig. 2 for d = 3 mm, with z and r denoting streamwise and radial directions. The measurements denote the boundary of the blue portion of the flame, and are terminated where yellow soot luminosity prevents observation of the blue boundary. The small change of flame shape as the pressure varies shows that effects of buoyancy are small. The comparison between predictions and measurements is reasonably good, including lengths, widths and the tendency of the flames to attach below the burner exit, for a range of burner exit Reynolds numbers. Predicted

108

and measured temperature distributions of ethylene/air flames at 0.25 atm. and $z/d = 39.2$ are illustrated in Fig. 3. Temperatures were measured with thermocouples corrected for radiation errors. The comparison between predictions and measurements is good except for a slight overestimation of peak temperatures and underestimation of flow widths.

It is useful to consider flame residence times, t_r, defined as the time for a fluid parcel to convect along the axis from the burner exit to the flame sheet, in order to interpret smoke point flame lengths. Predictions of t_r for nonbuoyant flames as flame lengths are varied for a particular burner diameter are illustrated in Fig. 4. They show that t_r is proportional to L, which differs from behavior when the boundary layer approximations apply, considered by Glassman [17], due to effects of streamwise diffusion. Similar predictions when the burner diameter is varied for a particular flame length appear in Fig. 5. They show a progressive increase of t_r with burner diameter, which differs from ng conditions where t_r is relatively independent of burner diameter [14]. Another feature of these results is the large residence times of nonbuoyant flames in comparison to buoyant flames of comparable size (an order of magnitude larger) which implies rather different soot reaction conditions.

Soot Properties. A typical example of soot volume fraction distributions in nonbuoyant jet diffusion flames is illustrated in Fig. 6. These results are for an acetylene flame with an ambient oxygen mass fraction of 0.75, d = 3 mm, Re = 250 and p = 0.25 atm. An annular soot layer is evident near the burner exit with soot building up near the axis as the flame tip (ca. $z/d = 9.35$) is approached. Soot oxidation extends to the axis beyond the flame tip with soot concentrations becoming small far from the burner exit for this nonsooting flame. The breadth of the soot-containing region provides unprecedented spatial resolution in comparison to buoyant flames.

Laminar Smoke Points. Laminar smoke point flame lengths, L_s, were measured for ethylene/air and propane/air flames at pressures of 0.5, 1.0 and 2.0 atm. Some typical results for propane/air flames at atmospheric pressure at μg, and at ng from [14,16], are as follows:

d (mm)	1.6 (μg)	2.7 (μg)	5.9 (μg)	10.0 (ng)
L_s (mm)	42	38	42	162-169

Findings for ethylene/air flames were similar. There are several interesting features about the comparison between observations at μg and ng. First of all, the nonbuoyant flames exhibit laminar smoke point flame lengths, in contrast to the conjecture of Glassman [17], because their residence times vary with flame length as discussed earlier. Secondly, varying d at μg has little effect on L_s even though residence times vary appreciably. Additionally, the L_s are roughly four times shorter at μg than ng. Finally, residence times at the laminar smoke point are appreciably larger at μg than ng, 200-1500 ms in comparison to 40-50 ms. The different soot paths in nonbuoyant and buoyant flames, and the extended oxidation region of nonbuoyant flames, undoubtedly play a role in this behavior, although the specific mechanisms are unknown. These results clearly highlight the substantial differences between the global sooting properties of frequently studied buoyant diffusion flames and the nonbuoyant diffusion flames of greater practical importance.

Conclusions

Thus far, the major conclusions of the study are as follows: (1) the laminar-flamelet approach appears to be attractive for predicting the structure of soot-containing laminar diffusion flames; (2) residence times of nonbuoyant laminar diffusion flames (L/d < 20-30) increase proportional to burner diameter and flame length, with the latter behavior being caused by effects of streamwise diffusion; (3) nonbuoyant diffusion flames exhibit much broader soot-containing regions and

larger soot-oxidation regions in comparison to buoyant diffusion flames; and (4) the properties of laminar smoke point flame lengths and residence times of nonbuoyant laminar diffusion flames have little resemblance to those of more widely studied buoyant laminar diffusion flames.

References.

1. Cochran, T.H. and Masica, W.J., *Thirteenth Symposium (International) on Combustion*, The Combustion Institute, Pittsburgh, 1970, pp. 821-829.
2. Haggard, J.B. Jr. and Cochran, T.H., Combust. Flame, Vol. 5, 1972, pp. 291-298.
3. Edelman, R.B. et al., *Fourteenth Symposium (International) on Combustion*, The Combustion Institute, Pittsburgh, 1972, pp. 399-412.
4. Klajn, M. and Oppenheim, A.K., *Nineteenth Symposium (International) on Combustion*, The Combustion Institute, Pittsburgh, 1982, pp. 223-235.
5. Bahadori, M.Y., Edelman, R.B., Stocker, D.P. and Olson, S.L., AIAA J., Vol. 28, 1990, pp. 236-242.
6. Bahadori, M. Y., Stocker, D. P. and Edelman, R. B., AIAA Paper No. 90-0651, 1990.
7. Bahadori, M.Y., Edelman, R.B., Stocker, D.P., Sotos, R.G. and Vaughan, D.F., AIAA Paper No. 92-0243, 1992.
8. Santoro, R.J., Semerjian, H.B. and Dobbins, R.A., Combust. Flame, Vol. 51, 1983, pp. 203-218.
9. Santoro, R. J., Yeh, T. T., Horvath, J. J. and Semerjian, H. G., Combust. Sci. Tech., Vol. 53, 1987, pp. 89-115.
10. Dobbins, R.A. and Megaridis, C.M., Langmuir, Vol. 3, 1987, pp. 254-259.
11. Megaridis, C.M. and Dobbins, R.A., Combust. Sci. Tech., Vol. 66, 1989, pp. 1-16; *Ibid.*, Vol. 77, 1990, pp. 95-109.
12. Gore, J.P. and Faeth, G.M., *Twenty-First Symposium (International) on Combustion*, The Combustion Institute, Pittsburgh, 1986, pp. 1521-1531.
13. Gore, J.P. and Faeth, G.M., J. Heat Trans., Vol. 111, 1988, pp. 173-181.
14. Sivathanu, Y.R. and Faeth, G.M., Combust. Flame, Vol. 81, 1990, pp. 133-149.
15. Sivathanu, Y.R. and Faeth, G.M., Combust. Flame, Vol. 82, 1990, pp. 211-230.
16. Schug, K.P., Manheimer-Timnat, Y., Yaccarino, P. and Glassman, I., Combust. Sci. Tech., Vol. 22, 1980, pp. 235-250.
17. Glassman, I., *Twenty-Second Symposium (International) on Combustion*, The Combustion Institute, Pittsburgh, 1988, pp. 295-311.
18. Faeth, G.M., *Proceedings of AIAA/IKI Microgravity Science Symposium*, AIAA, Washington, 1991, pp. 281-293.
19. Dixon-Lewis, G. et al., *Twentieth Symposium (International) on Combustion*, The Combustion Institute, Pittsburgh, 1984, pp. 1893-1903.
20. Rogg, B., in *Mathematical Modeling in Combustion and Related Topics* (C.-M. Brauner and C. Schmidt-Laine, eds.), Martinus Nijhoff Publishers, Amsterdam, 1988, pp. 551-560.
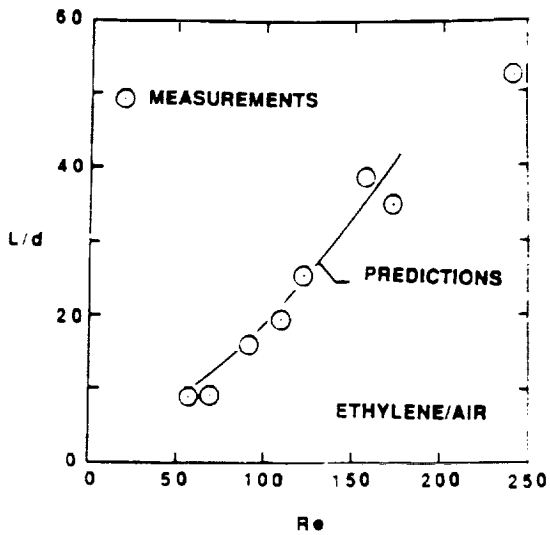
Fig. 1 Predicted and measured flame lengths of nonbuoyant ethylene/air jet diffusion flames. Measurements from Haggard and Cochran [2].
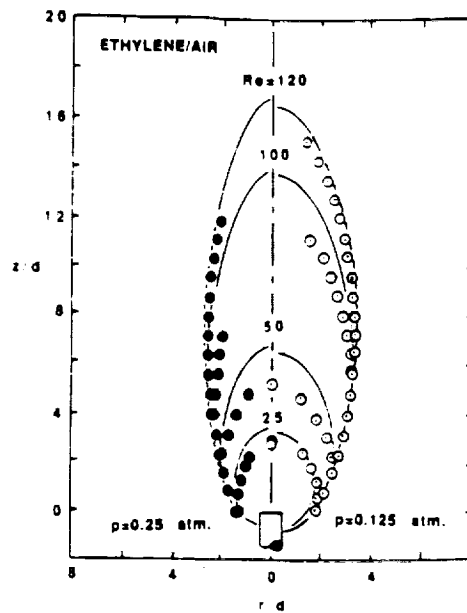
Fig. 2 Predicted and measured flame shapes of weakly-buoyant ethylene/air jet diffusion flames.
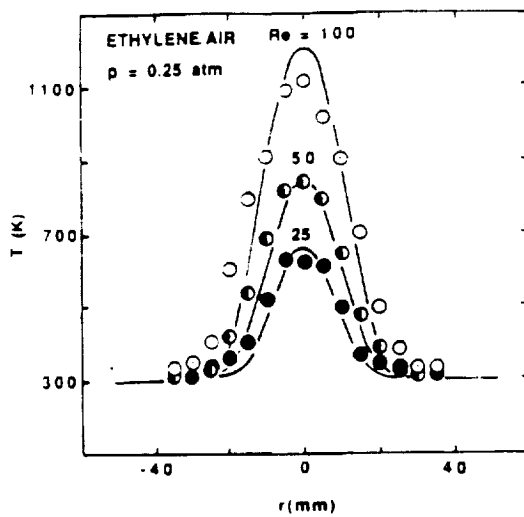

Fig. 3 Predicted and measured temperature distributions in weakly-buoyant ethylene/air diffusion flames.
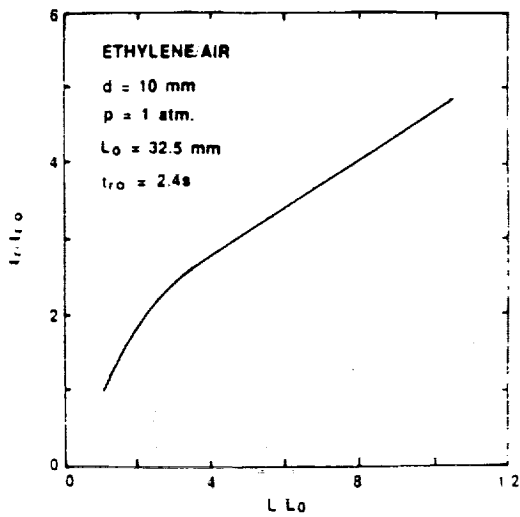
111

Fig. 4 Predicted flame residence times as a function of flame length for nonbuoyant ethylene/air diffusion flames.
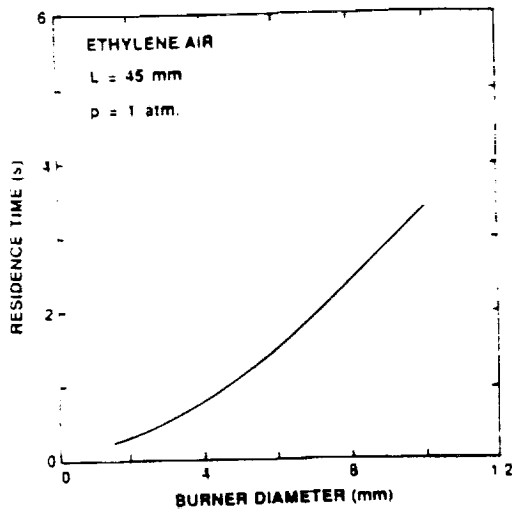

Fig. 5 Predicted flame residence times as a function of burner diameter for nonbuoyant ethylene/air diffusion flames.
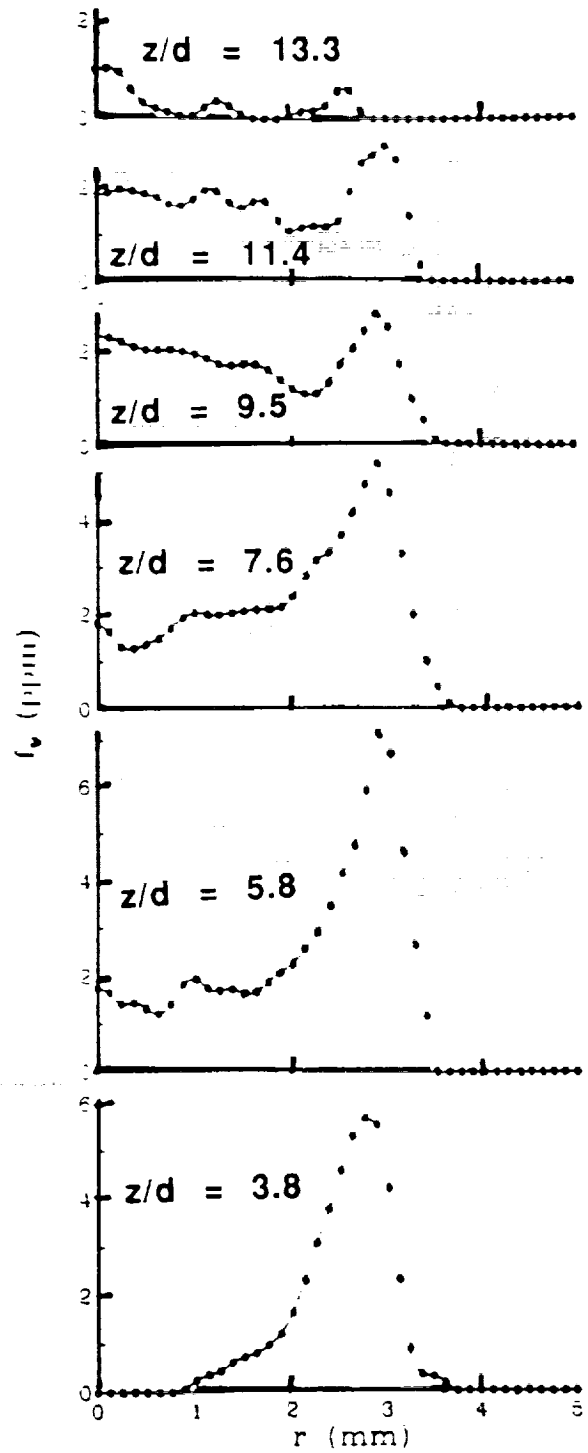

Fig. 6 Measured soot volume fraction distributions for weakly-buoyant acetylene/oxygen/nitrogen diffusion flames: d = 3 mm, Re = 250, p = 0.25 atm. and ambient oxygen mass fraction = 0.75.

112

COMMENTS

Question: (Osamu Fujita, Hokkaido University): (1) Are there any reasons why you choose ethylene as a fuel?

2) Are the flames you showed in the presentation steady-state or not? According to our results, width or diameter of butane flame become larger with increase in microgravity time, especially when the gas injected speed is low.

Answer: Our experiment currently involves ethylene and acetylene flames because they have been studied extensively in the past - particularly ethylene. Future work will address effects of fuel type over a broader range.

The low-pressure weakly-buoyant flames we are studying in the laboratory are all steady; we can operate them indefinitely and accumulate data over periods of hours. The low-gravity tests using the NASA KC-135 facility last 15-20 seconds, which yields stable flame lengths in the absence of disturbances, but are marginal as steady-state flames due to limited development times and disturbances. This is the best we can do prior to space-based tests at microgravity, but we don't believe that this compromises the major conclusions about differences of laminar smoke-point properties for nonbuoyant and buoyant flames.

Question (C.T. Avedisian, Cornell University): Can you comment on sensitivity of your predictions to uncertainties in physical property values?

Answer: Our predictions are sensitive to estimates of the radiative heat losses from the flames due to the strong variation of transport properties with temperature. Thus, we currently are working on additional measurements of the distribution of radiative heat losses from the flames to reduce these uncertainties. Computations for ad hoc variations of properties have been carried out to a limited degree, and suggest that reduced diffusivities yield proportional increases of flame lengths.